Appl. Phys. B 35, 59–64 (1984)

Applied Physics B Photophysics and Laser Chemistry

Chaotic Behavior of a Hybrid Optical Bistable System without a Time Delay

F. Mitschke

Institut für Quantenoptik, Universität, Welfengarten 1, D-3000 Hannover 1, Fed. Rep. Germany

N. Flüggen

Institut für Theoretische Physik, Universität, Appelstrasse 2, D-3000 Hannover 1, Fed. Rep. Germany

Received 24 April 1984/Accepted 14 June 1984

Abstract. The observation of chaos in a hybrid optical bistable device is reported. There is no delay line in this system. An investigation of the mechanism concentrates on a somewhat simplified structure. This structure is described by a third-order differential equation with quadratic nonlinearity. Its realization as an electronic circuit is studied in detail. As we observe patterns of universal behaviour, we also comment on the relation to iterative maps.

PACS: 42.65

The theory of chaos in iterated maps [1] has been applied to physical systems that have a time delay, or retardation, as a feature governing their temporal behaviour [2, 3]. However, many observations of chaos were done in continuous systems [4, 5] that are better described by a differential equation. In this paper we describe an electrooptical hybrid system without time delay exhibiting chaotic behaviour. Our approach for an understanding is to introduce certain approximations in order to come to a somewhat simplified structure. This structure is described by a third-order differential equation with quadratic nonlinearity, an electronic realization permits detailed studies.

1. The Hybrid Optical System and Its Model

We first turn to a description of the hybrid device. The experimental set-up is shown in Fig. 1a. Two plane mirrors forms a Fabry-Perot resonator with a finesse $\mathscr{F} \cong 8$. The mirror spacing of about 1 mm can be finely adjusted by means of a piezoelectric translator (PZT). The 1 mW beam of a 632 nm helium-neon laser is transmitted through the Fabry-Perot resonator and then monitored by a photo diode. Its signal is amplified, and an adjustable bias voltage is added. The loop is closed by feeding back the amplifier output signal to PZT. The resonator, placed at more than 1 m away from the laser, is tilted very slightly with respect to the light beam in order to avoid any undesired optical feedback into the laser. With a very small amplifier bandwidth (e.g., dc to 10 Hz), one finds bistability and hysteresis by scanning either the amplifier gain or the offset voltage. This should not require any further explanation. With larger bandwidth (dc to 1 kHz), a scan of the bias voltage over an Airy peak yields the following behaviour:

An oscillation of about 1550 Hz sets in and undergoes two period-doubling bifurcations. Next, a short interval of weakly chaotic motion is found with some islands of more or less stable subharmonic periodicities like period 3 ($P3$) or $P9$, but otherwise, no obvious structure is seen. Scanning on further, the fundamental $P1$ reappears, this time a few percent lower frequency. After bifurcations to $P2$, $P4$, and $P8$ (Fig. 2), a chaotic regime with an inverse sequence of band mergings is entered, where periodic windows like $P5$ or $P3$ are seen occasionally. Amplitudes grow steadily during this process, but eventually all oscillations stop when the system switches, or precipitates, to the low-

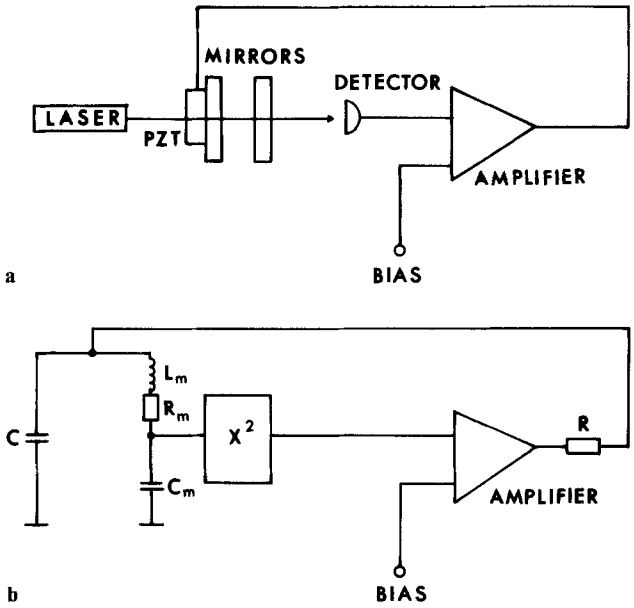

Fig. 1. (a) Set-up of the hybrid optical bistable device (PZT: piezoceramic translator). (b) The electronic model (X^2:squarer)

transmission state. A reversal of the scanning direction reveals that the first onset of oscillations is subject to a hysteresis. While the same is true for the point, where the chaos finally ends, all other events mentioned do not seem to have any hysteresis. No serious efforts were made to determine the convergence ratio δ of the bifurcations or the splitting ratio α of the amplitudes.

Measurements performed on the opened loop reveal that the time delay in the system is one order of magnitude shorter than the period of the fundamental oscillation $P1$ and should therefore play no major role. However, we find that PZT has a mechanical resonance, i.e. a damped-oscillatory approach to a new equilibrium position after a voltage step is applied. This resonance is characterized by its center frequency of 1550 Hz (which coincides with the frequency of $P1$) and its Q factor of about $Q=15$. It is this resonance of PZT together with the nonlinearity provided by the Airy peak that is able to produce chaotic motion.

In order to gain insight into the dynamic behaviour of the system, let us consider a somewhat simplified structure, as given in Fig. 1b. This electronic circuit models the hybrid device within certain approximations. PZT is replaced by its idealized equivalent circuit consisting of the components C, R_m, and L_m [6]. The latter three generate a resonance that models the mechanical characteristics, while C represents the electrical capacity of PZT. We assume that in steady state the PZT length is linearly dependent on the applied voltage. R stands for the output impedance of the amplifier. Note that the network for PZT contains three complex impedances and will thus lead to a differential equation of third order. The peak of the Airy function is here approximated by a quadratic parabola, generated by a squarer module. This is certainly a lowest-order approximation, that should not be expected to describe all the experimental details of the hybrid device. It is clear, for example, that bistability is not possible within the parabola approximation.

For technical reasons we consistently use a slightly modified version of the circuit throughout this paper. The modification consists of an interchange of the

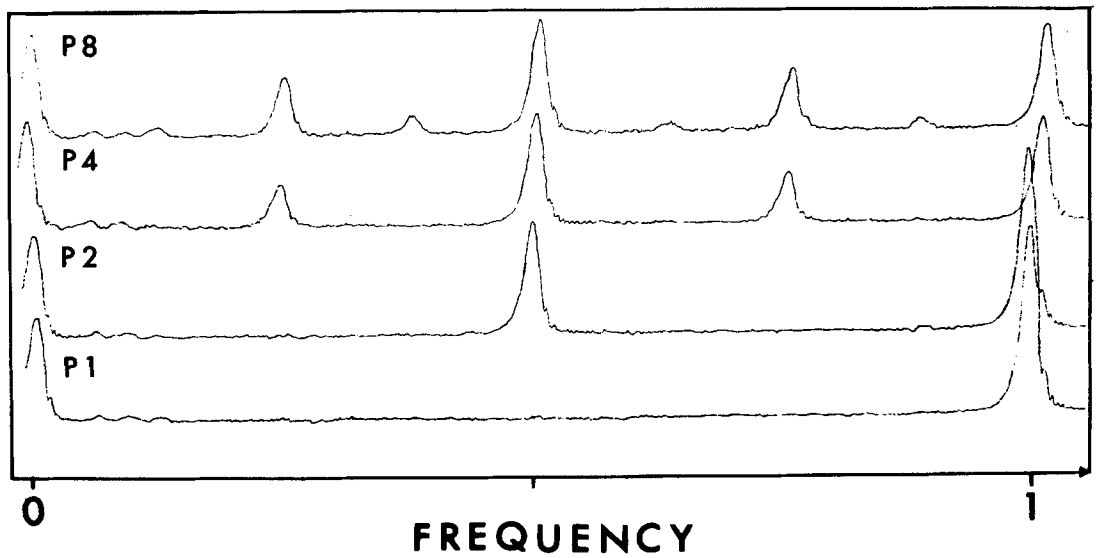

Fig. 2. Period doubling sequence in the hybrid device. The bias voltage was increased monotonously from $P1$ to $P8$. Vertical scale is approximately logarithmic. Spurious peaks at power line frequency and harmonics appear below $f=1/8$

amplifier with the squarer (U_{cm} is first amplified and then squared). This does not alter the patterns of behaviour, and both versions are seen to be equivalent by some simple rescaling. The dynamic range of the circuit, however, is considerably improved.

We now turn to a discussion of the equation describing the circuit. It is given by

$$\dddot{U}+\ddot{U}\left(\frac{L}{R}+R_mC\right)+\dot{U}\left(\frac{R_m}{R}+\frac{C}{C_m}+1\right)+\frac{1}{RC_m}U = \frac{v^2}{RC_m}(U-\mu)^2 \quad (1)$$

with $U=U_{cm}$, v: gain, μ: bias. Time is measured in units of $\omega^{-1}=(LC)^{1/2}$ and L, C, and C_m are scaled with ω. This differential equation contracts phase space volume V with a constant rate everywhere: $(1/V)dV/dt = L/R+R_mC$. The fixed points of the system are

$$U_{\text{fix}\pm}=\frac{1}{2v^2}(2v^2\mu+1\pm\sqrt{1+4v^2\mu}). \quad (2)$$

A linear stability analysis yields that $U_{\text{fix}+}$ is always unstable while $U_{\text{fix}-}$ is stable over a range of parameters. One can thus determine the first bifurcation.

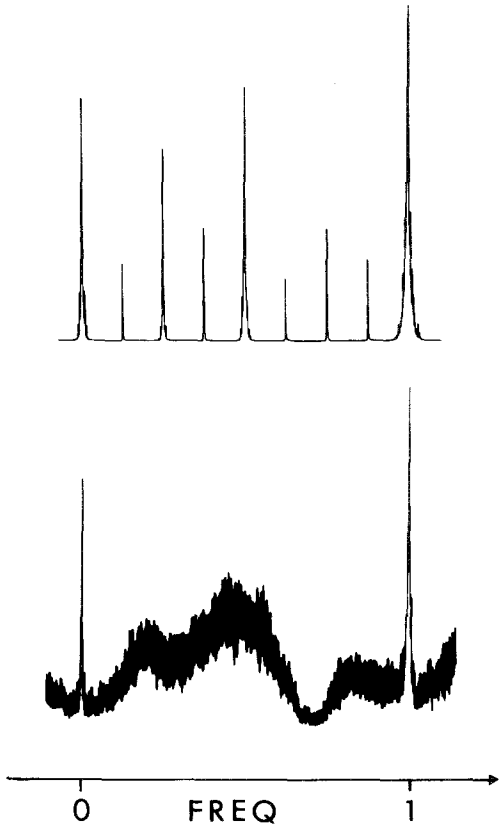

Fig. 3. Spectra obtained from the electronic device, with $R=1800\,\Omega$, $C=C_m$, $L=1268\,\Omega$, $v=1.158$, $\mu=3.634$, and $\omega=8.129\times10^4\,s^{-1}$. These two examples show $P8$ at $R_m=205\,\Omega$ (upper) and chaos at $R_m=181\,\Omega$. Vertical scale is approximately logarithmic

2. Experiments with the Electronic Model

We will now describe in some detail the experiments on the electronic circuit of Fig. 1b. They may be viewed at as calculations on an analog computer. In fact, we checked the accuracy of its solutions by comparison with runs of a digital computer. We found that the results typically agree to well within 1%. In terms of speed, however, the analog circuit is superior by several orders of magnitude. As we consider qualitative structures only, we do not attempt to simulate PZT quantitatively, but rather choose component values such as to yield a fundamental frequency of about 18 kHz. This high speed makes the study of the solutions on an oscilloscope screen very convenient. For a stress parameter we use either the amplifier gain, the bias voltage, or the damping resistor R_m. Essentially, all patterns of behaviour described below can be obtained by varying any of these. It is just for the sake of clarity that in the following description, we will refer to a R_m variation only.

For very high R_m, the system rests in the fixed point $U_{\text{fix}-}$. Decreasing R_m, one finds limit cycle oscillations and a sequence of period doubling bifurcations up to the onset of $P32$ (Fig. 4). We determine the convergence rate δ and find from a row of similar measurements $\delta_1=7.0\pm0.13$, as defined in [3], $\delta_2=4.64\pm0.13$, $\delta_3=4.6\pm0.5$ (δ_4 uncertain) which seems to fit well with the prediction for the one-dimensional logistic model that $\delta_\infty=4.669$. We also recorded spectra of the oscillations with a spectrum analyzer (Fig. 3). The evaluation of the average power in the spectral peaks is performed according to [7]. For the bifurcation from $P1$ to $P2$, power goes down by $2\beta=7$ dB, and for $P2$ to $P4$, we found about 12 dB. Averaging all other values from $P4$ to $P8$ and $P8$ to $P16$, we arrive at $2\beta=13.2\pm0.5$ dB. This is in excellent agreement with the theoretical prediction of 13.215 dB for the logistic model.

In the chaotic regime (Fig. 4) we find an inverse sequence of band mergings with a convergence ratio of 4.7 ± 0.6. We also observe more than ten periodic windows in this regime, the most prominent ones having $P6$, $P5$ (bifurcating into $P10$) and $P3$ (bifurcating into $P6$ and $P12$). The position of windows, their order of appearance and their itineraries, or patterns of visitation, are also consistent with the situation in one-dimensional maps [8] with only few exceptions that we are going to discuss below. If R_m is decreased more and more, an extra "hook" in the phase portrait appears and shifts towards $(U,\dot{U}) = (U_{\text{fix}+},0)$. We checked that simultaneously $\dot{U}$ and $\ddot{U}$ approach zero. At the moment the trajectory touches

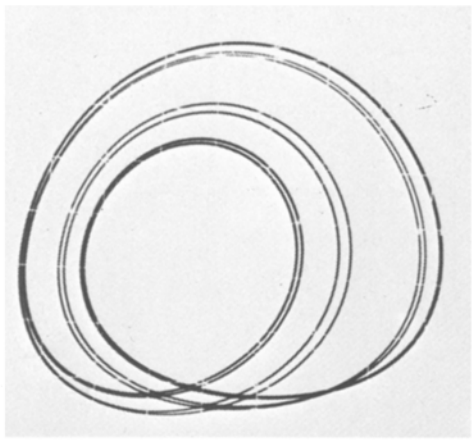

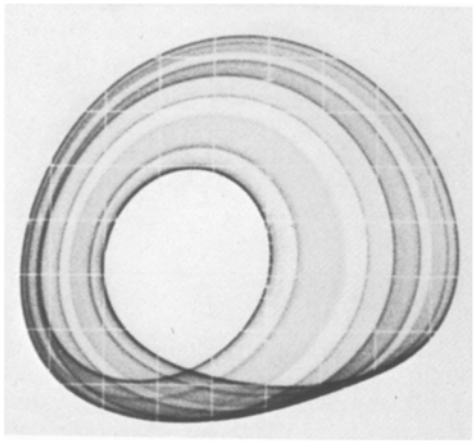

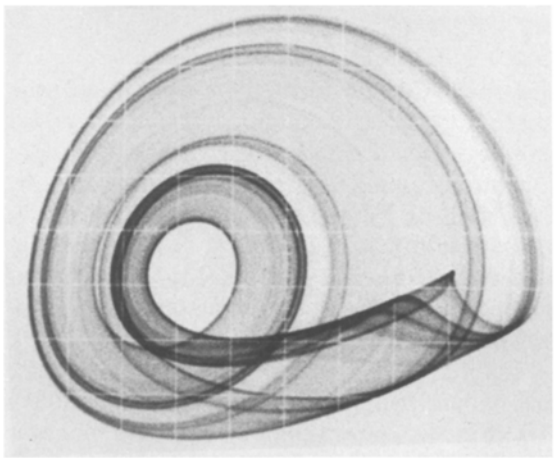

Fig. 4a–c. Phase portraits from the electronic device. U (horiz.) vs. $\dot{U}$ (vert.). Parameters as in Fig. 3, with R_m set at 205 Ω, 181 Ω, and 94 Ω, respectively

the unstable fixed point, the oscillations abruptly stop. This is an example of a boundary crisis [9]. The process corresponds with the switching to the low transmission state of the hybrid device. As there is no such state in the parabola approximation, the solution

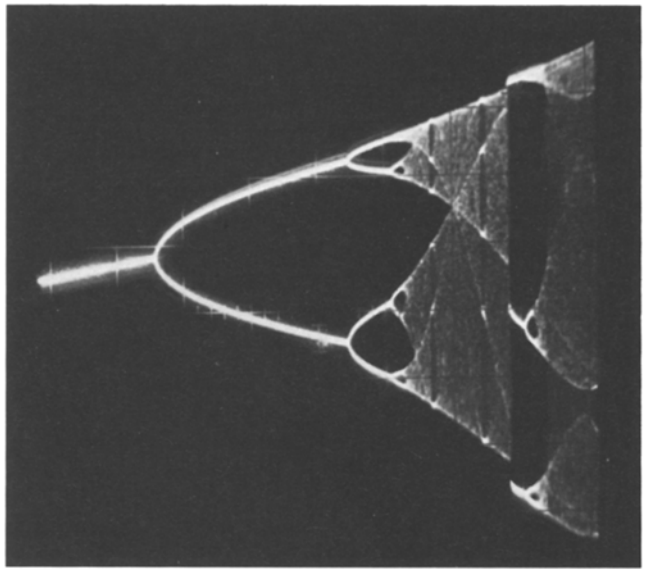

Fig. 5. Part of bifurcation diagram from the electronic system. Scan was from right to left

can go beyond all limits on a digital computer, while the analog system is limited by the supply voltage.

As one should expect a three-dimensional flow to behave like a two-dimensional rather than a one-dimensional mapping, we devoted some study to the deviation from the behaviour of the logistic equation. A first step to make them visible is a bifurcation diagram. We produced it by scanning the bias voltage with a ramp that also swept the horizontal deflection of an oscilloscope. The oscillations were fed into a sample-and-hold circuit, and the sampled voltage was given to the vertical channel of the escilloscope. Samples were taken at all negative-going zeroes in $\dot{U}$. The first obvious deviation is revealed at the first $P3$ window. A step in amplitude (Fig. 5) is accompanied by a hysteresis at the onset of this window (not visible in Fig. 5 as, for reasons of clearness, only one scan direction is shown). We mention that the two-dimensional Henon map [10], which also has the property of contracting the phase space volume with a constant rate everywhere, exhibits the same amplitude step and hysteresis at the $P3$ window if parameters are chosen for strong dissipation such as to make it resemble the logistic equation. Beyond the first $P3$ window, more deviations from the logistic model appear. We observe windows not consistent with [8], e.g. a second $P3$ window with an antiharmonic bifurcation to $P6$. The map describing our system is visible (at least in a projection to a lower-dimensional space) in a so-called return map. To construct it experimentally, takes two sample-and-hold circuits and some control logic. At defined phases of the oscillations, say whenever $\dot{U}$ has negative-going

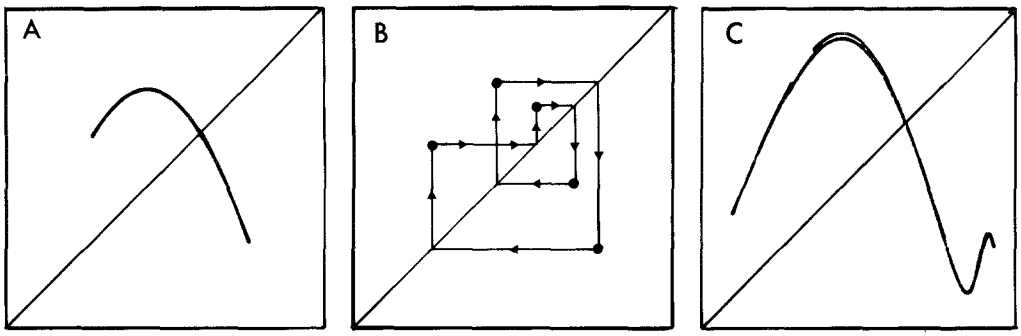

Fig. 6A–C. Return map of the electronic system: U_n (horiz.) vs. U_{n+1} (vert.). These examples are taken with parameters as in Fig. 3, with R_m at 181 Ω (A), 178 Ω (B), and 94 Ω (C). Case B is in the first $P5$ window. The arrows indicate how the mapping is iterated. The "splitting" visible in (C) is also existent but not resolved in (A), it becomes more pronounced and is seen to be a multiple folding when the phase space contraction rate is decreased as for Fig. 7

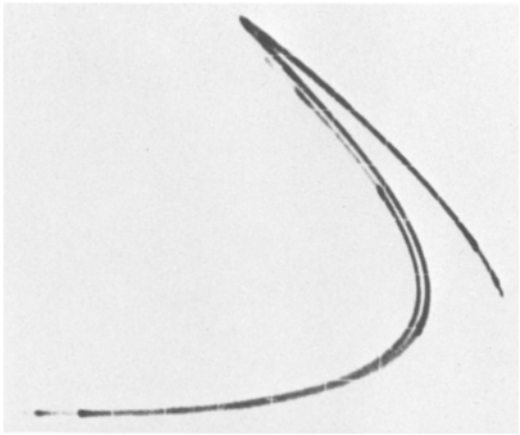

Fig. 7. Poincaré section. Parameters: $R=6400\,\Omega$, $v=2.372$, $\mu=3.033$, and $R_m=91\,\Omega$, otherwise as in Fig. 3

zeroes, trigger pulses are generated. By one of these pulses, the first sample-and-hold circuit is triggered, and at the subsequent pulse, this applies to the second one, while the first one keeps its sample. Both samples are fed to the horizontal and vertical channels of an oscilloscope, respectively, which is keyed bright after the second sample is taken. A display of U_n vs. U_{n+1} appears (Fig. 6). After a while the cycle starts from the beginning. It is, of course, also possible to display U_n vs. U_{n+m}, $m=2,3,4,\ldots$ by simple changes in the control logic. One finds that in regimes, where the logistic equation seems to describe the system quite well, the return map is, in fact, very nearly a quadratic parabola. For low R_m, however, more structure appears (Fig. 6C). This is the regime, where windows inconsistent with the logistic model appear.

We take another view of the map that describes our system by displaying its attractor. This is simply accomplished by producing a Poincaré section of the flow of our system. Experimentally, the easiest method is to display a phase portrait like Fig. 4 but to key the oscilloscope bright only for a short interval (50 ns), when $\ddot{U}$ has a defined phase, for example negative-going zeroes. Due to the fact that our system behaves nearly one-dimensional, this yields a figure which is hardly distinguishable from a line. We therefore increased R in order to decelerate phase space contraction (Fig. 7). Still, one has to take into consideration the brightness steps of the trace in order to appreciate the intricate, self-similar structure which is mostly obscured by the geometrical resolution of the image (even more so in reproduction).

3. Summary and Conclusion

We summarize that our hybrid electro-optical system follows a route to chaos that is, in parts, similar to a Feigenbaum route. Our electronic model reveals that, even within the simplifications made, the behaviour is quite complex. On the other hand, a variety of studies can be conducted in this system very conveniently which helps to gain an understanding of its behaviour. One may think of dropping the simplifications in future work and then conclude directly about the mechanisms in the more complicated hybrid device. For a technical motivation, let us just mention that our hybrid device is of exactly the same structure as a widely employed scheme for a laser frequency stabilization. This scheme uses an external Fabry-Perot resonator to generate an error signal, which is fed to a PZT that, in turn, moves an optical component in the laser resonator such as to correct the laser frequency. From a viewpoint of control systems engineering, it is certainly no surprise that resonances in this sort of applications must be cancelled or damped out carefully, as it has been known for a long time that feedback loops with resonances as well as those with time delays tend to oscillate. Our system shows quite clearly how the resonance contributes the degrees of freedom that are necessary for chaotic motion.

While our Eq. (1) belongs into a class of equations that has been considered a candidate for producing chaos before [11], we have demonstrated how it arises from an experiment. We believe, that our example is among the simplest autonomous continuous systems with chaotic behaviour that are relevant for physical experiments.

Acknowledgements. We thank Profs. W. Lange, H.-U. Everts, and H.-J. Mikeska for constant support and numerous valuable discussions.

References

1. E. Ott: Rev. Mod. Phys. **53**, 655 (1981) and references therein
2. R.H.G. Helleman: Am. Inst. Phys. Conf. Proc. **57**, 236 (1979)
3. H.M. Gibbs, F.A. Hopf, D.L. Kaplan, R.L. Shoemaker: Phys. Rev. Lett. **46**, 474 (1981)
   K. Ikeda, H. Daido, O. Akimoto: Phys. Rev. Lett. **45**, 709 (1980)
4. See, e.g., I. Testa, J. Perez, C. Jeffries: Phys. Rev. Lett. **48**, 714 (1982)
5. E. Lorenz: J. Atmosph. Sci. **20**, 130 (1963)
   See also: O.E. Rössler: Z. Naturforsch. **31a**, 259 and 1168 (1976)
6. See, e.g., W.G. Cady: *Piezoelectricity* (Dover, New York 1964)
7. M. Nauenberg, I. Rudnick: Phys. Rev. B **24**, 493 (1981)
8. N. Metropolis, M.L. Stein, P.R. Stein: J. Comb. Theory A **15**, 25 (1973)
9. C. Grebogi, E. Ott, J.A. Yorke: Phys. Rev. Lett. **48**, 1507 (1982)
10. M. Henon: Commun. Math. Phys. **50**, 69 (1976)
11. P. Coullet, C. Tresser, A. Arneodo: Phys. Lett. **72** A, 268 (1979)